Published in final edited form as:
J Dent Res. 2008 August ; 87(8): 701–709.

Mussel-designed Protective Coatings for Compliant Substrates

N. Holten-Andersen[1] and **J. H. Waite**[2,*]

1*Graduate Program in BioMolecular Science & Engineering, University of California at Santa Barbara, Santa Barbara, CA 93106, USA*

2*Marine Science Institute, University of California at Santa Barbara, Santa Barbara, CA 93106, USA*

Abstract

The byssus of marine mussels has attracted attention as a paradigm of strong and versatile underwater adhesion. As the first of the 3,4-dihydroxyphenylalanine (Dopa)-containing byssal precursors to be purified, *Mytilus edulis* foot protein-1 (mefp-1) has been much investigated with respect to its molecular structure, physical properties, and adsorption to surfaces. Although mefp-1 undoubtedly contributes to the durability of byssus, it is not directly involved in adhesion. Rather, it provides a robust coating that is 4-5 times stiffer and harder than the byssal collagens that it covers. Protective coatings for compliant tissues and materials are highly appealing to technology, notwithstanding the conventional wisdom that coating extensibility can be increased only at the expense of hardness and stiffness. The byssal cuticle is the only known coating in which high compliance and hardness co-exist without mutual detriment; thus, the role of mefp-1 in accommodating both parameters deserves further study.

Keywords

adhesion; byssus; coating; cuticle; hardness; mussel foot protein-1; Mytilus

INTRODUCTION

The oral environment has much in common with the wave-swept seashore. Both are naturally saline and endure dramatic variations in fluid flow, temperature, and pH; both are plagued by opportunistic microbes; and both are subject to relentless wear and abuse. The tissues of organisms facing these environments have evolved adaptations at multiple levels of organization to improve their function, but marine organisms have had the advantage of time, since their adaptations go back to long before the emergence of the first toothy vertebrates (Cox, 1969). Increasingly, structures made by intertidal marine invertebrates are undergoing scrutiny for their potential to inspire new paradigms in dental and biomedical technology (Carrington, 2008).

The National Institute of Dental and Craniofacial Research (NIDCR) has a tradition of funding interdisciplinary approaches to national health needs. The NIDCR's support of marine bio-adhesion, for example, goes back nearly 40 years (*e.g.*, Bowen *et al.*, 1974). This long-term investment has only recently begun to achieve practical rewards, and several transitioning breakthroughs in "mussel-inspired" adhesive technology have occurred in the past 18 months (Lee *et al.*, 2007a,b; Podsiadlo *et al.*, 2007). Adhesion, however, is only one of many potentially useful features of mussel byssus. Others include abrasion-resistant coatings, self-healing

*corresponding author, waite@lifesci.ucsb.edu

polymers, giant self-assembling mesogens, and pH-triggered cross-linking (Hassenkam *et al.*, 2004; Harrington and Waite, 2007; Holten-Andersen *et al.*, 2007).

Our purpose here is to review recent advances in the structure and function of one of the more than 20 known proteins of mussel byssus, namely, *Mytilus edulis* foot protein-1 (mefp-1). After a general description of the byssus, the review is organized to cover the following topics in order of presentation: (1) the byssal cuticle as the functional location of mefp-1, (2) mechanical and chemical properties of the cuticle, (3) biochemistry of mefp-1 and homologous proteins from other mussel species, (4) surface chemistry of mefp-1, (5) model of mefp-1 assembly in the cuticle, and (6) concluding remarks. For the sake of clarity and brevity, mussel-adhesive proteins are generically referred to as 'mfps' or mussel foot proteins, or, more specifically, as '*gs*fps', where the *gs* refers to the particular mussel genus and species, followed by a number (from 1 to 6) that reflects the order of discovery.

Mytilus edulis foot protein-1 (mefp-1), also known as "polyphenolic protein" and "mussel-adhesive protein", acquired a reputation for adhesion for both commercial and scientific reasons. Commercial suppliers of various grades of mfp-1 described their product (*e.g.*, CellTak™, Becton-Dickinson, Bedford, MA, USA) as an adhesive protein, because it improved attachment of cells and tissues in culture. More to the point, however, byssal-adhesive plaques exhibit the highest 3,4-dihydroxyphenylalanine (Dopa) levels in the byssus (Mascolo and Waite, 1986), and as recently as 1995, mefp-1 was the only known protein with a Dopa content high enough to be reconciled with the 15% Dopa levels at the plaque-substratum interface (Waite, 2002). Even in the recent monograph, *The Adhesive of the Blue Mussel* (Haemers, 2003), mefp-1 is the only protein discussed in any detail. With the introduction of soft ionization mass spectrometry and more aggressive extraction methods, however, additional Dopa-rich proteins have emerged. Two of these, mfp-3 and mfp-5, have Dopa contents in excess of 20 mol% and are localized exclusively to the adhesive plaques near the interface with the substratum (Papov *et al.*, 1995; Waite and Qin, 2001; Zhao *et al.*, 2006; Zhao and Waite, 2006). It is now quite evident that mefp-1 and related homologues in other mussel species have little to do with the adhesion of byssal plaques to substrata, but instead serve an important coating function. The aim of this review is to do justice to the actual function of mefp-1 and how that function relates to its structure and the development of novel coating technologies.

SOURCE OF INSPIRATION

Mussel Byssus

Mussel byssus has distinctive features that reflect its function as a holdfast (Fig. 1). Like spider silk, byssus is a biomacromolecular structure that is rapidly made to order as needed by the organism and consists of 3 distinct parts: stem, threads, and adhesive plaques. Emerging from living tissue at the base of the mussel foot is the byssal stem; from this emanate hundreds of byssal threads, each of which ends in a flattened plaque specialized for adhesion. Byssal threads are made from an assortment of extracellular matrix proteins and assembled outside the confines of living tissue (Waite, 2002;Waite *et al.*, 2004). Given the number of reviews on byssus (Carrington, 2002;Waite *et al.*, 2005;Wiegemann, 2005;Silverman and Roberto, 2007), it will suffice here to say that the major structural protein of the threads is an exotic collagenous block co-polymer having a central collagen core that is flanked with either silk or elastin-like domains. Because of the manner in which the silk- and elastin-collagen copolymers are distributed in each byssal thread, the exposed distal end is typically about 10 times stiffer than the proximal end (Waite *et al.*, 2002,2004). Both distal and proximal portions are surprisingly extensible (≥ 75%); however, most of the strain occurs after a recoverable yield point and contributes significantly to high hysteresis and toughness of byssal threads (Gosline *et al.*, 2002;Carrington and Gosline, 2004).

Byssal Cuticle

The outer surface of byssal threads is coated by a thin (5 μm) but distinctive cuticle in *Mytilus* (Vitellaro-Zuccarello, 1981)—the distinctive feature being the presence of densely packed mottled granules in *Mytilus edulis* and *M. galloprovincialis* byssal cuticles. Viewed by scanning electron microscopy (SEM), the cuticle on *M. galloprovincialis* mussel threads resembles sandpaper (Fig. 2a). In thin sections for transmission electron microscopy (TEM), the mottled granules, which are embedded in a continuous homogeneous matrix, reveal a distinct biphasic structure (Fig. 2b), a feature that is greatly enhanced when viewed by atomic force microscopy (AFM) (Fig. 2c). The granules are ~0.8 μm in diameter and constitute about 50% of the cuticle volume. The phase-separated morphology within each granule has a domain size of 20-40 nm. The cell and molecular processes mediating formation of this unusual microstructure remain unknown, but some cautious conjecture is offered later in this review.

Mechanical Properties

The hardness (H) and stiffness (E_i) of the hydrated cuticle coating *M. galloprovincialis* threads have been measured by nanoindentation (Holten-Andersen *et al.*, 2005, 2007). These parameters are of particular interest, because $H^{3/2}/E$ is empirically proportional to wear resistance in ceramics (Bhushan, 1999). Consistent with its function to protect the collagens in the core, cuticle H and E_i are comparable with those of engineering epoxies (Unnikrishnan and Thachi, 2006) (Table 1). Note that H and E_i of the cuticle are 4-5 times higher than those of the core collagens. Despite its high stiffness, the cuticle remains extensible, with a tensile failure strain as high as 70% (Holten-Andersen *et al.*, 2007). Large-scale catastrophic failures (such as in Fig. 2a) are prevented from propagating through the cuticle at strains less than 70% by controlled micro-tearing localized to the interface between the granules and the matrix and within the matrix itself. In other words, single detrimental macroscopic failures of the cuticle have been replaced by multiple non-detrimental micro-tears. The granular composite coating thereby “absorbs” strain-induced damage by redistributing it to a large volume, thereby enabling coat strains up to 70% before rupture (Holten-Andersen *et al.*, 2007). Micro-tears are presumed to be reversible, since threads can be repeatedly extended with no apparent structural changes.

The significance of the micro-granular structure in strain tolerance is corroborated by the results of two comparative investigations. The cuticle on *P. canaliculus* threads is homogeneous instead of granular; despite having H and E_i similar to those of the *M. galloprovincialis* cuticle, it shattered at strains of 30% or lower (Holten-Andersen *et al.*, 2007). Moreover, the cuticle of *M. californianus*, with granule diameters at only 200 nm (25% of those in *M. galloprovincialis*), exhibits catastrophic cracking only at strains greater than 120% (Holten-Andersen and Waite, unpublished observations).

Cuticle Composition

Only one protein, mfp-1, is known to be present in the byssal cuticle. This protein is derived from the accessory gland of the mussel foot. *In situ* hybridization of mussel foot sections with gene-specific primers based on mfp-1 and PCR has localized the expression of mfp-1 to the accessory gland, which lines both sides of the ventral groove from the base of the foot to within a few millimeters of the foot tip (Miki *et al.*, 1996). Furthermore, with both Dopa and dihydroxyproline as specific markers for mfp-1, mfp-1 has been demonstrated to be distributed over the entire length of the accessory gland and byssal thread in *M. galloprovincialis* (Sun and Waite, 2005). The distinctive mottled granular structure of the cuticle is also evident in the accessory gland where the granules are produced and stockpiled prior to secretion (Vitellaro-Zuccarello, 1981). Perhaps related to the physical and chemical inertness of the mature cuticle, immunohistochemical localization of mfp-1 in the cuticle has been less than satisfactory in quality (Benedict and Waite, 1986). Apparently, epitopes in mfp-1 are lost

during its rapid chemical maturation. Indeed, mfp-1 in *D. polymorpha* (Dpfp-1) ceased to cross-react with specific polyclonal antibodies within 20 min of secretion from the foot (Anderson and Waite, 2000).

Besides protein, significant amounts of fatty acids (8% w/w) have been detected in byssal threads of *M. edulis* (Cook, 1970) and *M. galloprovincialis* (Holten-Andersen *et al.*, unpublished observations). Other known constituents are metal ions such as Fe, Al, Si, and Ca. Recent energy-dispersive x-ray spectroscopic analyses of threads detected elevated metal levels in the byssal cuticle (Sun and Waite, 2005), and in a previous study with metal-binding stains, Fe was found to be localized to the cuticle (Coulon *et al.*, 1987). In the case of Fe, it is clear from *in vitro* experiments that mefp-1 binds tightly to Fe^{III}, but the extent to which metal in byssus reflects specific placement or adventitious deposition related to environmental pollution remains to be resolved. Titanium oxide from effluents, for example, found its way into the cuticle of *M. galloprovincialis* byssus (Coulon *et al.*, 1987), but has never been detected in byssal threads from pristine waters. Even in this, questions regarding the manner of deposition remain: Is the metal actively incorporated by the mussel or adsorbed by passive exchange between seawater and byssus? The metal composition of byssus appears to be highly variable and often reflects the chemistry of the water column and/or sediment. When Fe^{III} was added to seawater as $FeCl_3$, its passive uptake by byssal threads was not measurable (Sun and Waite, 2005). However, when live mussels were introduced to $FeCl_3$-enhanced seawater, the new threads they produced had a cuticle enriched in iron (Sun and Waite, 2005). Wilker's group (Sever *et al.*, 2004) has detected Fe^{III} in byssal threads by electron paramagnetic resonance spectroscopy and proposed a time-dependent redox exchange. The functional significance of iron binding is still in question, since many byssal threads of mussels collected from the field are devoid of iron, but seem mechanically robust in tension (Sun and Waite, unpublished observations). In particular, the effects of metals on the mechanical properties of byssal cuticle need to be investigated.

Mfp-1 Biochemistry

Primary Structure—As the primary cuticular protein and first byssal protein to be isolated from *M. edulis*, mefp-1 has undergone much scrutiny (Waite and Tanzer, 1981). Its characterization has presented many challenges to protein purification, including oxidative instability, incompatibility with sodium dodecylsulfate, irreversible binding to most chromatographic media at neutral pH, aggregation tendencies, unstable epitopes, and many exotic post-translational modifications (Waite, 1983; Waite *et al.*, 1985). Effective purification strategies now exist for mefp-1 and are directly applicable to mfp-1s from most other species (Waite, 1995).

Mefp-1 has a pI of 10.3 (Waite, 1983) and a mass of about 110 kDa, as determined by both MALDI TOF mass spectrometry (Taylor *et al.*, 1996) and sedimentation equilibrium (Deacon *et al.*, 1998). Despite many attempts, it has not been possible to crystallize mefp-1; however, useful insights about the shape of mefp-1 in solution have emerged from analysis by sedimentation velocity centrifugation. The frictional coefficient *f*, a shape factor, can be estimated from the sedimentation coefficient *s*, since $s = M(1-v\rho)/[Nf]$, where M is mass, v is partial specific volume, ρ is density of medium, and N is Avogadro's number. By solving for *f* and dividing by the calculated f_o for a perfect sphere (from Stokes' equation $f = 6\pi\eta R$, where η is medium viscosity and R is radius of a dry sphere having the same M as in the equation for *s*), one can estimate how much the protein deviates from a spherical shape, *e.g.*, f/f_o approaches a minimum of 1 for a sphere. Assuming that mefp-1 shares the hydration of 0.35 g H_2O/g protein typical for globular proteins, the frictional ratio f/f_o of 3.2 would predict an aspect ratio *a/b* of 45 for a prolate ellipsoid (Deacon *et al.*, 1998). This shape, however, is not consistent with the 10-nm hydrodynamic radius measured by dynamic light-scattering (Haemers *et al.*,

2005), because 0.22 nm is not a meaningful *b* dimension for the protein. Instead, the 10-nm radius is more suggestive of a flexible coil. If we allow mefp-1 to be represented by a flexible coil where $a/b = 1$, then a much higher hydration of 25 g H_2O/g protein is calculated from $f/f_o = 3.2$, according to Perrin's equation (Deacon *et al.*, 1998). Such high hydration would not be inconsistent with the composition of mefp-1 in which nearly every amino acid is either naturally polar (Lys, Ser, Thr, Tyr) or rendered polar by post-translational modification (Hyp, Dopa), as amplified below.

The amino acid composition of mefp-1 contains, on average, 10 mol% of each of the following amino acids: Ala, Pro, Ser, Thr, Tyr, *trans*-4 hydroxyproline (Hyp), *trans* 2, 3- cis 3, 4-dihydroxyproline (diHyp), and Dopa. The most abundant residue, Lys, occurs at 20 mol%. Upon trypsin digestion, purified mefp-1 readily degrades like a string of beads into a closely related family of decapeptides. The consensus decapeptide sequence is AKPSYP**P*TY*K, where P* denotes *trans*-4-hydroxyproline, P** 2, 3-*trans*-3, 4-*cis*-dihydroxyproline, and Y* 3, 4-dihydroxyphenylalanine (Waite *et al.*, 1985; Taylor *et al.*, 1994a) (Fig. 3).

Two complete mefp-1 variant sequences have been deduced from cDNA and consist of short non-repetitive amino termini 70-90 amino acids long, followed by a decapeptide sequence repeated many times in tandem (Fig. 3). The consensus decapeptide, AKPSYPPTYK, occurs about 71 times, interrupted 13 times by the hexapeptide AKPTYK (Filpula *et al.*, 1990;Laursen, 1992).

Mfp-1s from nearly 20 other mussel species have been isolated and partially characterized (*e.g.*, Rzepecki *et al.*, 1991). Like mefp-1, they are classified by adding the first letter of the genus and species to fp-1. Only half a dozen sequences are known from both Edman- and cDNA-deduced sequences (Table 2). All but one of these (*Perna viridis*) contain significant Dopa, and all are dominated by Lys and Pro (though not always Hyp). In *Perna viridis*, Dopa is replaced by a modification of Trp (Zhao and Waite, unpublished observations). Only slight variations occur in the consensus sequences of mfp-1 from other *Mytilus* species—*M. californianus* and *M. galloprovincialis*—but the post-translational modifications are identical. Interestingly, only the sequences from *Mytilus* species appear to be associated with granular cuticles.

Higher-order Structure—Circular dichroism (CD) is probably the single most powerful tool for studying solution protein secondary structure. CD of mefp-1 under native and denaturing conditions exhibits a molar ellipticity that is consistent with ~70% random coil ([θ] minimum at 190 nm and maximum at 220 nm). Ellipticity was not detectably altered in native or recombinant mefp-1 by the addition of 6 M guanidine hydrochloride and/or heat (Williams *et al.*, 1989; Hwang and Waite, unpublished observations). The CD spectra of extremely stable polyproline II structures, such as collagen, resemble those of extended coils, but these melt with heat or denaturants (Greenfield, 2006). NMR studies of synthetic mefp1-inspired decapeptides such as AlaLysProSerTyrHypHypThrDopaLys suggest a bent left-handed helix (Olivieri *et al.*, 1997; Kanyalkar *et al.*, 2002); however, few of these constructs are faithful to all of the modifications present (Taylor and Weir, 2000). An increasingly popular notion is that the structure of mefp-1 in solution is limited to short stiff segments (bent helices) separated by flexible ones (Haemers *et al.*, 2005).

Redox and Metal-binding Chemistry—Mefp-1 is distinguished from typical proteins by many features; nothing, however, distinguishes it more than the Dopa content, approaching 10-15 mol%. In aerated solution at pH 7, Dopa has a redox potential $E_o = +0.65$ V, in which two half-reactions are coupled: $1/2O_2 + 2e + 2H^+ \leftrightarrow H_2O$ and Dopa ↔ Dopaquinone + 2e + $2H^+$. The oxidizing power of O_2 effectively drives the production of Dopaquinone at mid to higher pH levels. The Dopa-oxidase activity of mushroom tyrosinase can be harnessed to

accelerate oxidation by O_2 *in vitro* (Marumo and Waite, 1986; Burzio and Waite, 2000; Taylor, 2002); not surprisingly, byssal threads contain intrinsic Dopa oxidase activity (Waite, 1985). *In vitro*, the kinetics of mefp-1 oxidation by other oxidants, such as periodate or I_2, has been studied (Haemers *et al.*, 2003).

The oxidation of Dopa residues in mefp-1 to dopaquinones is a critical factor in protein cross-linking (Burzio and Waite, 2000), but does not guarantee it. The formation of diDopa, which occurs in byssus (McDowell *et al.*, 1999), proceeds from a two-electron oxidation of Dopa to dopaquinone (Fig. 4). The latter, however, needs another Dopa to give up one electron by reverse dismutation to produce 2 Dopa semi-quinones, which ultimately couple to form the diDopa cross-link. Haemers *et al.* (2003) have investigated the stoichiometry of this process: When k_{ox} exceeds k_{dis}, the remaining reducing equivalents are insufficient to reduce enough quinones to semi-quinones for cross-link formation. Recently, another cross-link, 5-S-cysteinylDopa, has been characterized from mussel byssus (Zhao and Waite, 2005, 2006). In contrast to diDopa, this arises by a Michael addition of the thiolate anion to dopaquinone, and hence is not dependent on semi-quinones. Thiol addition is the fastest known reaction involving quinones (Sternson *et al.*, 1973), but, given the low to trace levels of cysteine in most mussel byssi and mfp-1s, does not appear to be widely distributed.

A recent report suggests that the tendency for Dopa oxidation in mefp-1 is inversely correlated with osmotic pressure (van der Leeden, 2005). Since osmotic pressure affects protein conformation, this may be relevant to the redox stability of mefp-1 during confined storage in secretory granules *and* in the mottled granules of the cuticle.

The remarkable affinity of catechols, including Dopa, for metal ions has been recognized for some time (Martell and Sillen, 1982). The cumulative log stability constants (K_S) of metal-catecholate complexes are particularly high for Fe, Al, Si ($K_S > 40$). A comparable affinity for Fe^{III} by mefp-1 and its Dopa-containing peptides was demonstrated electrochemically to consist of the tris-catecholato-Fe^{III} form at low iron-to-protein ratios (Taylor *et al.*, 1994b), switching to a μ-*oxo*-bridged di-iron biscatecholate at higher concentrations (Taylor *et al.*, 1996). Curiously, no apparent cooperative effects in iron-binding were observed, despite the over 75 Dopas *per* mefp-1 molecule (Taylor *et al.*, 1994b). Wilker's group (Monahan and Wilker, 2004; Sever *et al.*, 2004) has made a specialty of studying the effects of iron-binding on extracted mussel foot proteins; however, the relevance of their results to mefp-1 function in byssus is difficult to assess, given the heterogeneity of their preparations. One noteworthy result, however, is that analysis of Fe^{III}-containing byssus by electron paramagnetic resonance indicates that high-spin Fe^{III} may be contributing to the accumulation of an organic free radical ($g = 1.997$ and 3249 G) that resembles Dopa semi-quinone (Sever *et al.*, 2004). This one-electron oxidation of Dopa by Fe^{III} could be an alternative route to cross-link formation *in vitro* and in the byssus (Monahan and Wilker, 2004). However, if both Fe^{II} redox-linked and catecholoxidase-dependent cross-linking occurs in byssus, the adaptive advantage for such redundancy is not yet apparent.

The formation of stable metal ion catecholate complexes is not limited to solution chemistry. Catechol complexation of minerals such as alumina (McBride and Wesselink, 1988), anatase (TiO_2) (Rodriguez *et al.*, 1996), borax (Harris *et al.*, 2007), iron oxide (Xu *et al.*, 2004), and possibly hydroxyapatite (Chirdon *et al.*, 2003) is well-known and has been exploited in affinity chromatography. Lee *et al.* (2006) were the first to quantify the energy of interaction between a single tethered catecholate (Dopa) and a metal oxide surface (TiO_2) using AFM. The interaction energy of the Dopa-Ti bond was calculated to be about half that of a covalent bond, yet was completely reversible for thousands of break/reformation cycles (Fig. 5). Although the byssal cuticle contains no detectable mineral, this finding nevertheless has considerable

significance for mefp-1, in that, when metals mediate interactions between the proteins in the cuticle, these interactions are likely less energetic than covalent cross-links, but reversible.

Surface Behavior

The widely assumed involvement of mfp-1 in mussel adhesion has made it a popular candidate for protein-adsorption studies. The mode of mefp-1 adsorption is strongly influenced by Dopa oxidation, backbone flexibility, and protein concentration. At pH 4-5 and ionic strength = 0.1 M, due to diminished Dopa oxidation and high positive charge density, mefp-1 chains are prevented from interacting in solution. Under these conditions, the initial adsorption of mefp-1 to surfaces conforms well to monolayer formation according to the Langmuir equation, $d\Gamma_1/dt = J_1B_1(1-\theta)$, where $d\Gamma_1/dt$ is the amount adsorbing *per* unit time, J_1 is the flux, B_1 is the sticking probability, and $(1-\theta)$ is the fraction of empty surface (Haemers *et al.*, 2002). On all tested surfaces exposed to mefp-1, B_1 is typically 1.0, and saturation is achieved in minutes (Fant *et al.*, 2000; Suci and Geesey, 2001b; Haemers *et al.*, 2002). For example, saturated adsorption of mefp-1 to a non-polar surface (methylterminated alkyl thiolated gold) occurred within 5-10 min and resulted in a hydrogel-like film 20 nm thick that contained nearly 94 weight% trapped water (Höök *et al.*, 2001). Periodate oxidation of Dopa and subsequent cross-linking condensed the film to 5 nm without decreasing its protein content. In contrast, mefp-1 adsorption to silica surfaces resulted in films with comparable amounts of protein, but with much higher initial stiffness and only moderate changes in stiffness and viscosity following oxidation (Fant *et al.*, 2000). Resistance of mefp-1 films on highly oriented pyrolytic graphite to shear with an AFM cantilever tip has been explored before and after Dopa oxidation (Hansen *et al.*, 1998). A ten-fold-higher shearing force was required to displace the film after a 20-minute treatment with catecholoxidase. The suggestion that mefp-1 films are susceptible to dehydration effects that depend on both cross-linking and surface interactions needs to be further explored.

Haemers *et al.* (2002) also examined mefp-1 adsorption to quartz at higher pH (6-8) under conditions where some Dopa oxidation was allowed to occur *prior* to mefp-1 adsorption. With light-scattering to monitor changes in hydrodynamic radius, it appeared that, at low mefp-1 concentrations (< 0.1 mg/mL), the radius decreased due to intramolecular cross-link formation and resulted in fewer surface contacts and the deposition of a stiffer film during mefp-1 adsorption. In contrast, at higher mefp-1 concentrations, the cross-links formed by Dopa oxidation were largely intermolecular, and the adsorbed aggregated protein was attached by numerous surface contacts and developed into rather compliant films (Haemers *et al.*, 2002). Although initial monolayer deposition still occurred at pH 6 to 8, the resulting adsorption isotherms deviated significantly from the Langmuir equation, in that the amount of mefp-1 adsorbed plotted against time exhibited multiple slopes and inflection points, both indicative of multilayer formation. Contributing factors for the slower adsorption rates to the initial monolayer were proposed to be lower flux J_2, lower sticking probability B_2, and a capacity for more mefp-1 adsorption that is contingent on a conformational change in the underlying monolayer (Haemers *et al.*, 2002). Only mefp-1 concentrations (> 0.1 mg/mL) with oxidized Dopa were observed to undergo deposition of additional layers, *i.e.*, adlayers, to the initial adsorbed mefp-1 (Haemers *et al.*, 2002).

The effect of oxidation on the comparative adsorption of mefp-1 and mefp-2 to germanium has been investigated by attenuated total reflection Fourier transform infrared (ATR FTIR) spectroscopy. Individually, both proteins exhibited similar trends with respect to surface coverage and adsorption rate constants (Suci and Geesey, 2001a). When introduced in succession with laminar flow, however, mefp-1 adsorbed to the exclusion of mefp-2 in a concentration-dependent manner. When mefp-1 was oxidized by periodate following adsorption, then mefp-2 adsorption levels approached those of mefp-1 itself, presumably by

adlayer formation (Suci and Geesey, 2001b). Probably, Dopa conversion to dopaquinone in adsorbed mefp-1 provided favorable sites for mefp-2 attachment. These results support the notion that mefp-1 adsorbs rapidly and irreversibly to a variety of surfaces. The effects of oxidation prior to adsorption are concentration-dependent and, at concentrations > 0.1 mg/mL, result in extensive protein aggregation and adlayers. When Dopa is oxidized after adsorption, film stiffness increases, as does adlayer deposition.

Until 2006, the role of Dopa in mefp-1 films following adsorption had been assumed to be largely a cohesive one. That is, Dopaquinone was thought to mediate formation of strong interactions, such as diDopa cross-links between mefp-1 molecules leading to film condensation (water loss) and film stiffness. Strong interactions are not limited to Dopa-mediated covalent cross-links, but include organometallic interactions as well. AFM force mode studies of mefp-1 suggest that the protein supports adhesion between the cantilever tip and surface, as measured by “jump-outs” (Frank and Belfort, 2002). The magnitude and range of the jump-outs were greatly enhanced by multivalent cations, namely, Mg, Ca, and Fe. The results with Fe^{III} are not surprising in view of strong Fe-chelation by Dopa; catecholate chelation of Mg and Ca, in contrast, is considerably lower (Martell and Sillen, 1982), but we can think of no other available interactions between divalent cations and a strongly basic protein besides perhaps those involving dihydroxyproline, whose chelating ability in mefp-1 remains untested.

More significantly, force-mode AFM, with a single Dopa residue tethered by its side-chain to the cantilever, demonstrated that Dopa is capable of contributing to a diverse range of surface interactions, including (a) covalent bonds following oxidation on a polyamine surface, (b) coordinate complexes on TiO_2 (Fig. 5), and (c) van der Waals forces on gold (Lee *et al.*, 2006). Notably, the interaction energy arising from the coordination of Dopaquinone with TiO_2 was reduced by more than 80% from that of Dopa (Lee *et al.*, 2006). Clearly, for strong adhesion and adsorption to metal oxide surfaces, it is desirable to have many Dopa residues and to prevent their oxidation to Dopaquinone. This is exactly the situation with respect to mcfp-3 and mcfp-5 in the adhesive plaque (Zhao *et al.*, 2006;Zhao and Waite, 2006).

Surface Forces Apparatus-A New Perspective

Although the surface forces apparatus (SFA) has many of the same attractive features as the AFM, including picoNewton sensitivity and nanometer extension, it is ideally suited for studying the interfacial behavior of molecules when more than one surface is involved. Typically, the SFA measures the repulsive or attractive forces during the approach and/or separation of 2 pristine (or modified) mica surfaces between which a microdroplet of analyte has been introduced. In the normal direction, the adhesion force $F_{ad} = WA/\delta$, where W is the adhesion energy, A is the contact area, and δ is the bridging length at break. With mefp-1 as analyte, the protein adsorbed strongly to the mica surfaces, but it exhibited repulsion on approach and lacked jump-outs on separation (Lin *et al.*, 2007). In contrast, mefp-3, an adhesive protein from the byssal plaque, immediately formed bridges between both mica surfaces that required a separation of 30 Å and a peak force of 3-4 mNewtons/m to break. Interpretation of these results suggests that whereas mefp-3 spontaneously adsorbs and bridges between surfaces, mefp-1 adsorbs only as a coating (Fig. 6). Only the application of considerable shear, which damaged or changed the conformation of mefp-1, induced it to switch from a coating to a bridging mode (Lin *et al.*, 2007). The effect of shear is reminiscent of the change in conformation in adsorbed mefp-1 before adlayer formation (Haemers *et al.*, 2002). The standard model of macromolecules adsorbing by loops, tails, and trains to surfaces predicts that loops and tails typically provide opportunities for bridging. Future studies need to explore whether mefp-1 fails to bridge on surfaces other than mica and, if so, whether this means that mefp-1 adsorbs without loops and tails.

Model of Assembly

The native cuticle in *Mytilus* species exhibits impressive prowess as a coating for a compliant substratum. Given the complex architecture of the cuticle, purified mfp-1 by itself is unlikely to provide the same performance. In combination with other molecules, however, such as metal ions, polyanions, and fatty acids, the outcome could be dramatically different. Metal ions in coordination with ligands such as Dopa tethered to larger macromolecules provide a fascinating alternative to covalent cross-linking. As already mentioned, the coordinate bond is about half as strong as the covalent, but is also reversible (Lee *et al.*, 2006). Moreover, in the right environment, non-innocent ligands like Dopa, complexed to redox-active metals (Fe^{III}, Cu^{II}, etc.), can give rise to cross-links by way of coupled free-radical intermediates. The formation of reversible micro-tears in the cuticle during extension may involve the breakage and re-formation of interactions between metal ions and Dopa in mfp1. This bears a striking similarity to the "sacrificial bonds and hidden lengths" model proposed for Ca^{2+}-mediated interactions in other biomolecular materials (Thompson *et al.*, 2002; Fantner *et al.*, 2005).

Of equal importance is a biochemical basis for the phase separation occurring in the mottled granules of *Mytilus* cuticles. In this regard, Vitellaro-Zuccarello's (1981) observation—that the granules and continuous matrix in fixed sections of the accessory gland exhibited differential lability to protease treatment—suggests the presence of different proteins or different forms of the same protein. This needs to be more systematically studied. The widespread occurrence of waxy outer layers in the exposed structures of living organisms and the fatty acid content of the byssus (Cook, 1970) are suggestive that *Mytilus* cuticle may be a composite of mfp-1 and fatty acids.

The extended structure and the high positive charge-density of mfp-1 make it an appropriate partner for spontaneous aqueous phase-separation with negative counterions, as observed in other biological systems (Waite *et al.*, 2005; Zhao *et al.*, 2005). Fatty acids may provide anionic partners for mfp1, with mfp-1 and Ca^{+2} acting as the macro- and micro-counterions, respectively, combining with negative fatty acids in an electrostatically driven self-assembly process. This is strongly reminiscent of the lipid-organizing role of myelin basic protein in the myelin sheath (Hu *et al.*, 2004; Marsh and Pali, 2004). Interestingly, a similar strategy is used for driving self-assembly of synthetic polyelectrolytes and surfactant (Antonietti and Conrad, 1994; Antonietti *et al.*, 1995; Ober and Wegner, 1997), and the resulting material microstructures in these synthetic self-organizing systems appear surprisingly similar to those in the mussel cuticle.

CONCLUDING REMARKS

Despite the above-mentioned gaps in our understanding, the availability of mefp-1 and synthetic mefp-1-inspired decapeptides has spurred numerous initiatives in surface science. There is general agreement that: (1) mfp-1 adsorbs rapidly and strongly to a variety of surfaces; (2) the strength of adsorption is closely linked to the presence of dopa; (3) the oxidation of dopa before adsorption leads to weaker adsorption to mineral surfaces, but to stronger interactions with other organic macromolecules; and (4) the oxidation of dopa after adsorption provides an effective platform for adlayer formation. These features probably apply to all dopa-containing proteins and polymers (*e.g.*, Suci and Geesey, 2001a), whatever their function. A more subtle and distinguishing feature of mefp-1 has emerged from studies with the surface forces apparatus. The study by Lin *et al.* (2007) is a sobering reminder that adsorption is not necessarily a measure of adhesive ability. Mefp-1 adsorbs strongly to mica surfaces, but as a coating, not an adhesive.

Minimalist approaches in which only mfp-1-inspired decapeptides AKPSYPPTYK are used to tether large synthetic polymers to surfaces have also been informative. For example, Dalsin

et al. (2002, 2005) used the decapeptide (with Dopa-9) to bind polyethylene glycol (PEG) as a non-fouling film to gold and titanium oxide surfaces, and showed that such surfaces remained up to 98% free of fibroblasts over the extended test period. Although the simpler and more cost-effective Dopa showed a similar trend on TiO_2, on gold, PEG-tethered Dopa conferred a performance no better than the PEG-Tyr analog and much poorer than the decapeptide. Despite the economic advantages of Dopa tethers, the differences between Dopa and decapeptide are worth exploring. Does the decapeptide present Dopa more favorably to the surface? Does it offer better protection against oxidation? Is Dopa in the decapeptide more or less shielded from solvation? Does the decapeptide adsorb as a train?

In common with most materials in wear, compliant materials need protection against abrasion. The mismatch in stiffness between compliant substrates and conventional coatings leads inevitably to catastrophic rupture when the coating is extended beyond its strain capacity; obviously, rupture voids any protective effects. The mfp-1-based cuticle, particularly in the byssus of *Mytilus* species, is 4-6 times harder and stiffer than the collagens it covers, yet it resists catastrophic rupture up to strains of 70% and beyond. Byssal cuticles with a granular micro-architecture exhibit the highest strain capacity, because they tolerate extensive but reversible micro-tearing within the matrix and at the matrix-granule interface. Films of pure mefp-1 do not possess a granular architecture and are unlikely to exhibit both high hardness and strain capacity. A most important goal of future work would be to identify the contributions of other components, such as the metal ions and fatty acids, to the mechanics and microstructure of mefp-1 films.

ACKNOWLEDGMENTS

We thank Drs. Frank Zok, Mieke van der Leeden, Peter Suci, and an anonymous reviewer for their insights. A grant from the National Institute of Dental and Craniofacial Research (5 R01 DE 014672) provided support for the work.

REFERENCES

Anderson KE, Waite JH. Immunolocalization of Dpfp1, a byssal protein of the zebra mussel *Dreissena polymorpha*. J Exp Biol 2000;203(Pt 20):3065–3076. [PubMed: 11003818]

Antonietti M, Conrad J. Synthesis of very highly ordered liquid crystalline phases by complex formation of polyacrylic acid with cationic surfactants. Angew Chem Int Ed Engl 1994;33:1869–1870.

Antonietti M, Burger C, Effing J. Mesomorphous polyelectrolyte-surfactant complexes. Adv Mater 1995;7:751–753.

Benedict CV, Waite JH. Location and analysis of byssal structural proteins of *Mytilus edulis*. J Morphol 1986;189:171–181. [PubMed: 3018262]

Bhushan, B. Principles and applications of tribology. John Wiley & Sons; New York: 1999.

Bowen JH, Mitchell PWD, Der Ohannessian T. Dental cement from marine sources. Final Report NIH 1974;70-2238:1–26.

Burzio LA, Waite JH. Cross-linking in adhesive quinoproteins: studies with model decapeptides. Biochemistry 2000;39:11147–11153. [PubMed: 10998254]

Carrington E. The ecomechanics of mussel attachment:from molecules to ecosystems. Integ Comp Biol 2002;42:846–852.

Carrington E. Along the silkroad, spiders make way for mussels. Trends Biotechnol 2008;26:55–57. [PubMed: 18191258]

Carrington E, Gosline JM. Mechanical design of mussel byssus: load cycle and strain rate dependence. Am Malacol Bull 2004;18:135–142.

Chirdon WM, O'Brien WJ, Robertson RE. Adsorption of catechol and comparative solutes on hydroxyapatite. J Biomed Mater Res Appl Biomater B 2003;66:532–538.

Cook, M. Composition of mussel and barnacle deposits at the attachment interface. In: Manly, RS., editor. Adhesion in biological systems. Academic Press; New York: 1970. p. 139-150.

Coulon J, Truchet M, Martoja R. Chemical features of mussels in situ exposed to an effluent. Ann Inst Oceanogr 1987;63:89–100.

Cox, LR. General features of Bivalvia. In: Moore, RC., editor. Treatise on invertebrate paleontology. 1. Geological Society of America; Kansas: 1969. p. N109-N121.

Dalsin JL, Hu BH, Lee BP, Messersmith PB. Mussel adhesive protein mimetic polymers for the preparation of nonfouling surfaces. J Am Chem Soc 2002;125:4253–4258. [PubMed: 12670247]

Dalsin JL, Lin L, Tosatti S, Vörös J, Textor M, Messersmith PB. Protein resistance of titanium oxide surfaces modified by biologically inspired mPEG-DOPA. Langmuir 2005;21:640–646. [PubMed: 15641834]

Deacon MP, Davis SS, Waite JH, Harding SE. Structure and mucoadhesion properties of mussel glue protein in dilute solution. Biochemistry 1998;37:14108–14112. [PubMed: 9760246]

Fant C, Sott K, Elwing H, Höök F. Adsorption behavior and enzymatically or chemically induced cross-linking of a mussel adhesive protein. Biofouling 2000;16:119–132.

Fantner GE, Hassenkam T, Kindt JE, Weaver JC, Birkedal H, Pechenik L, et al. Sacrificial bonds and hidden length dissipate energy as mineralized fibrils separated during bone fracture. Nat Mater 2005;4:612–616. [PubMed: 16025123]

Filpula DR, Lee SM, Link RP, Strausberg SL, Strausberg RL. Structural and functional repetition in a marine mussel adhesive protein. Biotechnol Prog 1990;6:171–177. [PubMed: 1367451]

Frank BP, Belfort G. Adhesion of mefp1 on silica: ionic effects on biofouling. Biotechnol Prog 2002;18:580–586. [PubMed: 12052076]

Gosline JM, Lillie M, Carrington E, Guerette PA, Ortlepp CS, Savage KN. Elastic proteins: biological roles and mechanical properties. Phil Trans R Soc Lond 2002;357(B):121–132. [PubMed: 11911769]

Greenfield NJ. Using circular dichroism collected as a function of temperature to determine the thermodynamics of protein unfolding and binding interactions. Nat Protoc 2006;1:2527–2535. [PubMed: 17406506]

Haemers, S. The adhesive of the blue mussel—controlling cross-linking. DUP Press; Delft: 2003. p. 102

Haemers S, van der Leeden MC, Koper GJM, Frens G. Cross-linking and multilayer adsorption of mussel adhesive proteins. Langmuir 2002;18:4903–4907.

Haemers S, Koper GJM, Frens G. Effect of oxidation rate on cross-linking of mussel adhesive proteins. Biomacromolecules 2003;4:632–640. [PubMed: 12741779]

Haemers S, van der Leeden MC, Frens G. Coil dimensions of the mussel adhesive protein mefp-1. Biomaterials 2005;26:1231–1236. [PubMed: 15475052]

Hansen DC, Corcoran SG, Waite JH. Enzymatic tempering of a mussel adhesive protein film. Langmuir 1998;14:1139–1147.

Harrington M, Waite JH. Holdfast heroics: comparing the molecular mechanical properties of *Mytilus californianus* byssal threads. J Exp Biol 2007;210(Pt 24):4307–4318. [PubMed: 18055620]

Harris WR, Amin SA, Küpper FC, Green DH, Carrano CJ. Borate binding to siderophores: structure and stability. J Am Chem Soc 2007;129:12263–12271. [PubMed: 17850151]

Hassenkam T, Gutsmann T, Hansma P, Sagert J, Waite JH. Giant bent core mesogens in the thread forming process of marine mussels. Biomacromolecules 2004;5:1351–1355. [PubMed: 15244450]

Holten-Andersen N, Slack N, Zok F, Waite JH. Nano-mechanical investigation of the byssal cuticle, a protective coating of a bio-elastomer. Mater Res Soc Symp Proc 2005;841:R3.7.1–Y3.7.1.

Holten-Andersen N, Fantner GE, Hohlbauch S, Waite JH, Zok FW. Protective coatings on extensible biofibres. Nat Mater 2007;6:669–672. [PubMed: 17618290]

Höök F, Kasemo B, Nylander T, Fant C, Sott K, Elwing H. Variations in coupled water, viscoelastic properties, and film thickness of a Mefp-1 protein film during adsorption and cross-linking: a quartz crystal microbalance with dissipation monitoring, ellipsometry, and surface plasmon resonance study. Anal Chem 2001;73:5796–5804. [PubMed: 11791547]

Hu YF, Doudevski I, Wood D, Moscarello M, Husted C, Genain C, et al. Synergistic interactions of lipids and myelin basic protein. Proc Natl Acad Sci USA 2004;101:13466–13471. [PubMed: 15353595]

Inoue K, Odo S. The adhesive protein cDNA of *Mytilus galloprovincialis* encodes decapeptide repeats but no hexapeptide motif. Biol Bull 1994;186:349–355. [PubMed: 8043658]

Inoue K, Takeuchi Y, Takeyama S, Yamaha E, Yamazaki F, Odo S, et al. Adhesive protein cDNA sequence of the mussel *Mytilus coruscus* and its evolutionary implications. J Mol Evol 1996;43:348–356. [PubMed: 8798340]

Kanyalkar M, Srivastava S, Coutinho E. Conformation of a model peptide of the tandem repeat decapeptide in mussel adhesive protein by NMR and MD simulations. Biomaterials 2002;23:389–396. [PubMed: 11761158]

Laursen, R. Reflections on the structure of mussel adhesive proteins. In: Case, ST., editor. Results and problems in cell differentiation. Vol. 19. Biopolymers. Springer-Verlag; Berlin: 1992. p. 55-74.

Lee H, Scherer NF, Messersmith PB. Single-molecule mechanics of mussel adhesion. Proc Natl Acad Sci USA 2006;103:12999–13003. [PubMed: 16920796]

Lee H, Lee BP, Messersmith PB. A reversible wet/dry adhesive inspired by mussels and geckos. Nature 2007a;448:338–341. [PubMed: 17637666]

Lee H, Dellatore SM, Miller WM, Messersmith PB. Mussel inspired surface chemistry for multifunctional coatings. Science 2007b;318:426–430. [PubMed: 17947576]

Lin Q, Gourdon D, Sun CJ, Holten-Andersen N, Anderson TH, Waite JH, et al. Adhesion mechanisms of the mussel foot proteins mfp-1 and mfp-3. Proc Natl Acad Sci USA 2007;104:3782–3786. [PubMed: 17360430]

Marsh D, Pali T. The protein-lipid interface:perspectives from magnetic resonance and crystal structures. Biochim Biophys Acta 2004;1666:118–141. [PubMed: 15519312]

Martell, AE.; Sillen, LG. Stability constants of metal-ion complexes. The Chemical Society; London: 1982. Part II, Special Publ. 25

Marumo K, Waite JH. Optimization of hydroxylation of tyrosine and tyrosine-containing peptides by mushroom tyrosinase. Biochim Biophys Acta 1986;872:98–103. [PubMed: 3089286]

Mascolo JM, Waite JH. Protein gradients in byssal threads of some marine bivalve molluscs. J Exp Zool 1986;240:1–7. [PubMed: 3095484]

McBride MB, Wesselink LG. Chemisorption of catechol on gibbsite, boehmite and noncrystalline alumina surfaces. Environ Sci Technol 1988;22:703–708.

McDowell LM, Burzio LA, Waite JH, Schaefer J. REDOR detection of cross-links formed in mussel byssus under high flow stress. J Biol Chem 1999;274:20293–20295. [PubMed: 10400649]

Miki D, Takeuchi Y, Inoue K, Odo S. Expression sites of two byssal genes of *Mytilus galloprovincialis*. Biol Bull 1996;190:213–217. [PubMed: 8652732]

Monahan J, Wilker JJ. Cross-linking the protein precursor of marine mussel adhesives: bulk measurements and reagents for curing. Langmuir 2004;20:3724–3729. [PubMed: 15875406]

Ober CK, Wegner G. Polyelectrolyte-surfactant complexes in the solid state: facile building blocks for self-organizing materials. Adv Mater 1997;9:17–31.

Ohkawa K, Nishida A, Yamamoto H, Waite JH. A glycosylated byssal precursor protein from the green mussel Perna viridis with modified Dopa side-chains. Biofouling 2004;20:101–115. [PubMed: 15203964]

Olivieri MP, Wollman RM, Alderfer JL. NMR spectroscopy of map repeating peptide segment. J Pept Res 1997;50:436–442. [PubMed: 9440044]

Papov VV, Diamond TV, Biemann K, Waite JH. Hydroxyarginine-containing polyphenolic proteins in the adhesive plaques of the marine mussel *Mytilus edulis*. J Biol Chem 1995;270:20183–20192. [PubMed: 7650037]

Podsiadlo P, Liu Z, Paterson D, Messersmith PB, Kotov NA. Fusion of seashell nacre and marine bioadhesive analogs: high-strength nanocomposite by layer-by-layer assembly of clay and L-3, 4-dihydroxyphenylalanine polymer. Adv Mater 2007;19:949–955.

Rodriguez R, Blesa MA, Regazzoni AE. Surface complexation at the TiO2 (anatase) aqueous solution interface: chemisorption of catechol. J Colloid Interface Sci 1996;177:122–131. [PubMed: 10479423]

Rzepecki LM, Qin X, Waite JH, Lavin ME. Molecular diversity of marine glues: polyphenolic proteins from five mussel species. Mol Mar Biol Biotechnol 1991;1:78–88. [PubMed: 1845474]

Sever MJ, Weisser JT, Monahan J, Srinivasan S, Wilker JJ. Metal mediated cross-linking in the generation of a marine-mussel adhesive. Angew Chem Int Ed Engl 2004;43:448–450. [PubMed: 14735531] *erratum* in *Angew Chem Int Ed Engl* 43:2986, 2004

Silverman HG, Roberto FF. Understanding mussel adhesion. Mar Biotechnol 2007;9:661–681. [PubMed: 17990038]

Sternson AW, McCreery R, Feinberg B, Adams RN. Electrochemical studies of adrenergic neurotransmitters and related compounds. J Electroanal Chem 1973;46:313–321.

Suci PA, Geesey GG. Comparison of adsorption behavior of two *Mytilus edulis* foot proteins on three surfaces. Coll Surf 2001a;22:159–168.

Suci PA, Geesey GG. Use of attenuated total internal reflection Fourier transform infrared spectroscopy to investigate interactions between *Mytilus edulis* foot proteins at a surface. Langmuir 2001b; 17:2538–2540.

Sun C, Waite JH. Mapping chemical gradients within and along a fibrous structural tissue: mussel byssal threads. J Biol Chem 2005;280:39332–39336. [PubMed: 16166079]

Taylor CM, Weir CA. Synthesis of the repeating decapeptide unit of Mefp1 in orthogonally protected form. J Org Chem 2000;65:1414–1421. [PubMed: 10814103]

Taylor SW. Chemoenzymatic synthesis of peptidyl 3,4-dihydroxyphenylalanine for structure-activity relationships in marine invertebrate polypeptides. Anal Biochem 2002;302:70–74. [PubMed: 11846377]

Taylor SW, Waite JH, Ross MM, Shabanowitz J, Hunt DF. trans-2,3- cis- 3,4 Dihydroxyproline in the tandemly repeated consensus decapeptides of an adhesive protein from *Mytilus edulis*. J Am Chem Soc 1994a;116:10803–10804.

Taylor SW, Luther GW, Waite JH. Polarographic and spectro-photometric investigation of Fe(III) complexation to DOPA-containing peptides and proteins from *Mytilus edulis*. Inorg Chem 1994b; 33:5819–5824.

Taylor SW, Chase DB, Emptage MH, Nelson MJ, Waite JH. Ferric ion complexes of a Dopa-containing adhesive protein from *Mytilus edulis*. Inorg Chem 1996;35:7572–7577.

Thompson JB, Kindt JH, Drake B, Hansma HG, Morse DE, Hansma PK. Bone indentation recovery time correlates with bond reforming time. Nature 2002;414:773–776. [PubMed: 11742405]

Unnikrishnan KP, Thachi ET. Toughening of epoxy resins. Design Monomers Polym 2006;9:129–152.

Van der Leeden MC. Are conformation changes, induced by osmotic pressure, the underlying mechanism. Langmuir 2005;21:11373–11379. [PubMed: 16285813]

Vitellaro-Zuccarello L. Ultrastructural and cytochemical study on the enzyme gland of the foot of a mollusc. Tissue Cell 1981;13:701–713. [PubMed: 6800062]

Waite JH. Evidence for a repeated DOPA- and hydroxyproline containing decapeptide in the adhesive protein of the mussel *Mytilus edulis*. J Biol Chem 1983;258:2911–2915. [PubMed: 6298211]

Waite JH. Catecholoxidase in the byssus of the common mussel. J Mar Biol Assoc UK 1985;65:359–371.

Waite JH. Precursors of quinone-tanning: dopa containing proteins. Methods Enzymol 1995;258:120.

Waite JH. Adhesion à la Moule. Integ Comp Biol 2002;42:1172–1180.

Waite JH, Qin XX. Polyphosphoprotein from the adhesive pads of *Mytilus edulis*. Biochemistry 2001;40:2887–2893. [PubMed: 11258900]

Waite JH, Tanzer ML. Polyphenolic substance of *Mytilus edulis*: novel adhesive containing L-dopa and hydroxyproline. Science 1981;212:1039–1040.

Waite JH, Housley TJ, Tanzer ML. Peptide repeats in a mussel adhesive protein: theme and variations. Biochemistry 1985;24:5010–5014. [PubMed: 4074674]

Waite JH, Vaccaro E, Sun CJ, Lucas JM. Elastomeric gradients: a hedge against stress concentration in marine holdfasts. Phil Trans R Soc Lond 2002;357(B):143–153. [PubMed: 11911771]

Waite JH, Lichtenegger HC, Stucky GD, Hansma P. Exploring the molecular and mechanical gradients in structural bioscaffolds. Biochemistry 2004;43:7653–7662. [PubMed: 15196007]

Waite JH, Holten-Andersen N, Jewhurst SA, Sun CJ. Mussel adhesion: finding the tricks worth mimicking. J Adhesion 2005;81:297–317.

Wiegemann M. Adhesion in blue mussels (*Mytilus edulis*) and barnacles (genus Balanus): mechanisms and technical applications. Aquatic Sciences 2005;67:166–176.

Williams T, Marumo K, Henkens R, Waite JH. Mussel glue protein has an open conformation. Arch Biochem Biophys 1989;269:415–422. [PubMed: 2493214]

Xu C, Xu K, Gu H, Zheng R, Liu H, Zhang X, et al. Dopamine as a robust anchor to immobilize functional molecules on the iron oxide shell of magnetic nanoparticles. J Am Chem Soc 2004;126:9938–9939. [PubMed: 15303865]

Zhao H, Waite JH. Coating proteins: structure and cross-linking in Fp-1 from the green shell mussel *Perna canaliculus*. Biochemistry 2005;44:15915–15923. [PubMed: 16313194]

Zhao H, Waite JH. Linking adhesive and structural proteins in the attachment plaque of *Mytilus californianus*. J Biol Chem 2006;281:26150–29158. [PubMed: 16844688]

Zhao H, Sun C, Stewart RJ, Waite JH. Cement proteins of the tube-building polychaete *Phragmatopoma californica*. J Biol Chem 2005;280:42938–42944. [PubMed: 16227622]

Zhao H, Robertson NB, Jewhurst S, Waite JH. Probing the adhesive footprints of *Mytilus californianus byssus*. J Biol Chem 2006;281:11090–11096. [PubMed: 16495227]

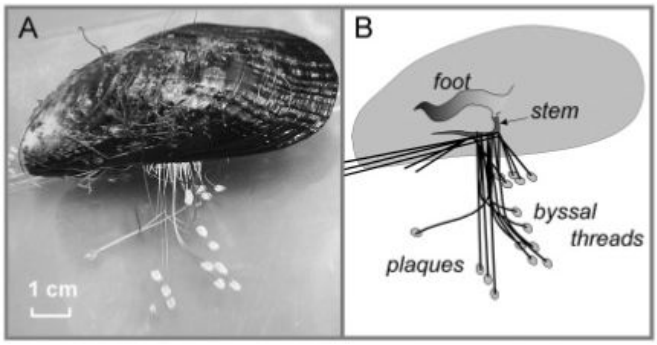

Figure 1.
A mussel attached by a byssus to glass **(A)** and a cartoon of the same mussel on the half-shell **(B)**, showing the relationship of the foot, stem, threads, and attachment plaque.

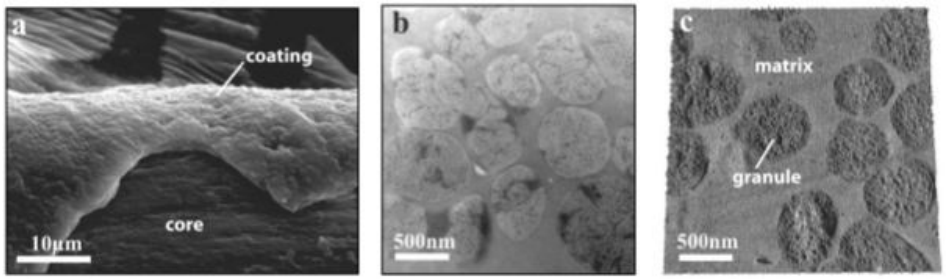

Figure 2.

Microstructure of mussel byssal cuticle. **(a)** SEM of *M. galloprovincialis* distal thread with partial delamination of cuticle, exposing the underlying collagenous core. **(b)** TEM of transverse cross-section of *M. galloprovincialis* distal thread cuticle, illustrating its granular composite morphology as well as the interior granular structure, osmium-tetroxide-stained for contrast. **(c)** AFM of untreated transverse cross-section of cuticle of *M. galloprovincialis* distal thread, confirming the observations made in TEM.

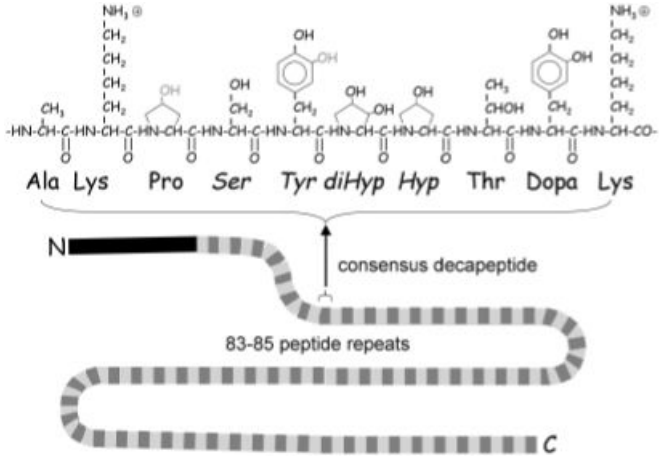

Figure 3.

Mytilus edulis foot protein (mefp-1) and the other mfp-1s are all highly repetitive proteins. The consensus repeat sequence in mefp-1 is a decapeptide. Lys-2, Tyr-5, Pro-6, Tyr-9, and Lys-10 are highly conserved. Residues Pro-6, Pro-7, and Tyr-9 are completely post-translationally hydroxylated. Conversion of Pro-3, Tyr-5 (gray), in contrast, is ≤ 30%. Mefp-1 contains a non-repetitive N-terminus, followed by mostly decapeptide and some hexapeptide sequences.

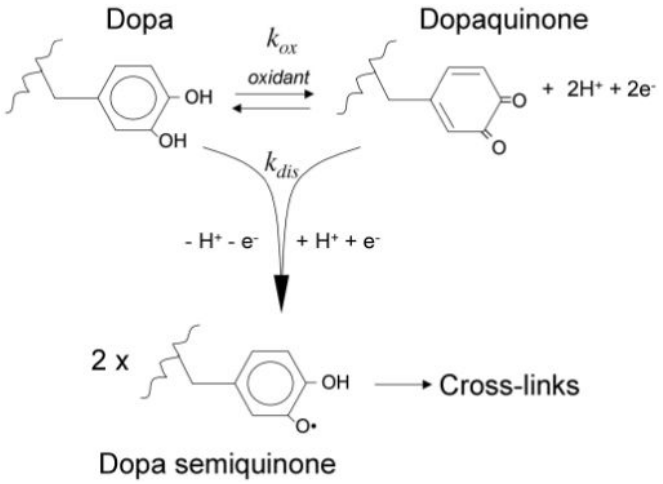

Figure 4.

Dopa side-chains of mfp-1 are susceptible to oxidation. A two-electron oxidation produces dopaquinone, which is able produce 2 semi-quinones by reverse dismutation with unreacted dopa. The Dopa semi-quinones can couple to produce di-dopa cross-links.

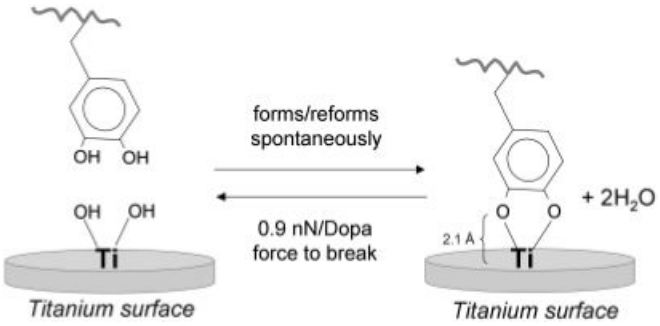

Figure 5.

Dopa side-chains in mfp-1s coordinate both soluble and insoluble metal oxides. Lee et al. (2006) have shown that the coordinate chelate bond between Dopa and a TiO_2 surface has half the interaction energy of a covalent bond, but re-forms spontaneously following breakage.

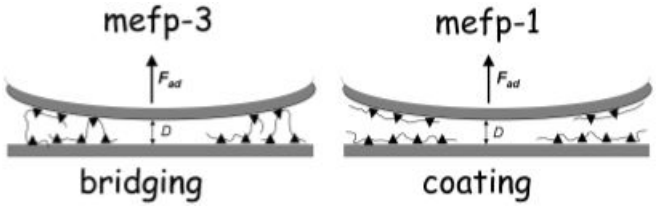

Figure 6.
Comparison of the behavior of mefp-1 and mefp-3 following introduction between 2 mica surfaces, as measured by the surface forces apparatus (Lin et al., 2007). Like a good adhesive, mefp-3 both coats and bridges the 2 mica surfaces; mefp-1, in contrast, only coats each surface.

Table 1

Comparison of Mean Stiffness and Hardness in *Mytilus* Cuticle, the Byssal Thread Core, and Synthetic Epoxies

	Hardness (MPa)	Stiffness (GPa)	Ultimate Strain (%)	Ref
Cuticle, Mytilus galloprovincialis	100 + 6.2 *n* = 7	1.7 + 0.1 *n* = 7	~70	Holten-Andersen et al., 2007
Collagen core, M. galloprovincialis	20 + 4.0 *n* = 7	0.4 + 0.09 *n* = 7	~75	Holten-Andersen et al., 2007
Synthetic epoxies	100-150	2-3	<5	Unnikrishnan and Thachi, 2006

Table 2

Repeat Sequence Motifs from mfp1s of Seven Marine Mussel Species (Italicized *P* and *Y* denote Pro and Tyr residues targeted for hydroxylation)

Species - mfp1	Mass, kDa	Sequence	Repeats	Reference
Mytilus edulis	108	AKPSYPPTYKAKPTYK	75	Laursen, 1992
			13	Filpula et al., 1990
Mytilus edulis	108	AK*P*SY*PP*T*Y*K	75	Laursen, 1992
		AKPTYK	13	Filpula *et al.*, 1990
M. galloprovincialis	~90	AK*P*SY*PP*T*Y*K	70	Inoue and Odo, 1994
M. californianus	~92	*P*KIS*YPPTY*K	64	Zhao and Waite, unpublished observations
M. coruscus		PKISYPPTYK	75	Inoue et al., 1996
Perna viridis	64	A*PPP*AXTAXK	14	Zhao and Waite, unpublished observations
		AT*PK*XTAXK	28	Ohkawa *et al.*, 2004
P. canaliculus	50	P*Y*VK	75	Zhao and Waite, 2005
Geukensia demissa	100	AK*PSPYVP*TG*Y*K	30	Laursen, 1992
		GQQKQTAYDPGYK		